Facile synthesis, x ray single crystal and optical characterizations of Cu-diphenylphosphino-methane organic crystalline semi-conductors

A. F. AL-HOSSAINY[*a], A. IBRAHIM[b]
[a]*Chemistry department, Faculty of Science - New valley, Assiut University, 71516 Assiut, Egypt*
[b]*Physics department, Faculty of Science, Tanta University, 31527 Tanta, Egypt*

In this paper, facile synthesis process of a new organic semiconductor single crystals $C_{38}H_{36}Cl_2N_2CuP_2$ (Cu-dppm) was reported. Single crystal X-ray structure determinations are recorded for cu-dppm (5a) complex, crystallize as poly crystalline form in the monoclinic space group $P2_1/n$ with a= 9.502(2) Å, b=8.128(3) Å, c=16.112(6) Å. In (Cu-dppm), the N(30)-C(31), C(34)-N(43) and N(43)-C(44) bond lengths could be categorized as one short (1.257 Å) and two long (1.472–1.475 Å) respectively. A short angle (71.756^0) of P(1)-Cu(17)-P(3) was observed. In addition, because of the growth process, a set of copper complexes were formed. Elemental analysis (EA), IR, ^{1}H-NMR, ^{31}P-NMR spectroscopic data and FAB mass spectra were used for more structural data analysis. The absorbance and transmittance spectra were measured for the obtained (Cu-dppm) organic complex (5a) over the incident photon energy range, 1.55-2.98eV (visible range wavelengths from λ= 400- 800 nm). The results of the absorptivity (ε_{max}=729.95 and 349.39 $Lmol^{-1}{}_{Cm}{}^{-1}$) were calculated in order to determine the optical band gap of Cu-dppm (5a) complex at λ_{mix} (436 and 580nm) respectively. The optical constant, i.e, refractive index of the organic semiconductor (5a) has been calculated as 1.265 at 2.86 eV.

(Received September 18, 2014; accepted November 13, 2014)

Keywords: $C_{38}H_{36}Cl_2N_2CuP_2$, IR, ^{1}H-NMR, ^{31}P-NMR spectroscopy, X-ray diffraction, Optical properties

1. Introduction

In the last few decades the search for new organic semiconductors single crystals with better properties have been increased because of their potential applications in various disciplines like microelectronics, semiconductors, sensors, laser technology. Organic materials are having inability to grow in large size and have impeded the use of single crystals of organic materials in practical device applications. In this regard, materials scientists focused their attention towards new semi organic crystals using organic compound with metal complexes in order to satisfy the present day technological requirements [1–3]. The interest in organic electronics is motivated by increasing the demands of supplementing Si-based electronics with materials that offer easier processing methods completed with functionalization by chemical manipulation. Their compatibility with lightweight, mechanically flexible plastic substrates, completed by new, innovative fabrication routes, makes them possible candidates for future electronic devices [4-7]. Moreover, due to different molecular tailoring possibilities via chemical synthesis, organic materials present an infinite variety in functionality.

The design of the molecular structures can be engineered to enhance particular properties (solubility in different solvents, color of light emission, crystal packing). In particular, addition of polar groups in polymers leads to rich systems for investigation of ferroelectricity [8]. By incorporating them in transistors (ferroelectric field-effect transistors-FeFETs), combined functionality can be achieved for non-volatile memory devices that are compatible with flexible plastic substrates [9]. Modification of the chemical end-groups also allows fabrication of large transistor arrays for organic sensors.

Different methods are developd to increase the sensitivity and selectivity of organic sensing transistors to different chemical or biological species [10]. Applications include environmental issues (e.g. air pollution), pH indicators, [11] food freshness, toxic compounds, stress and pressure indication in clothes [12]. Rapid progress is being made in the industrial development of the organic electronic devices. Organic devices can be implemented on large scale application area when their operation offer high performance, reliability, stability, long life time, good control and reproducibility. Impressive steps have been accomplished towards incorporation of organic conductors in devices [13].

Past investigations were hindered by material instabilities and structural defects that prevented the measurement and understanding of the intrinsic properties of the organic materials. Recently, careful design of new methods is achieved (both by electrostatic and chemical doping).That enabled the exploitation of the fascinating properties of carbon-based semiconductors, good control of the structural properties and charge density distribution in organic materials. In our previous work [14], organic semiconductor compound (Ni-dppm) shows typical semiconductor behavior. Optical properties of Ni-dppm complex were studied in the temperature range 77 to 300K.

In this work, the doping impact by Cu (5a) is reported for the dppm inorganic crystals. Facile synthesis, solubility study and growth of Cu-dppm of single crystal (5a) have

been done. In addition, the structural properties of Cu-dppm were analyzed by elemental analysis (EA), IR, ^{1}H-NMR, ^{31}P-NMR spectroscopic data and FAB mass spectra. Finally, the optically properties of the same compound are done.

2. Experimental setup and apparatus

2.1. Synthesis, solubility study and growth of single crystals

All the chemicals were obtained commercially and used without further purification. A mixture of 1:1 M ratio of acetyl acetone (1.002g, 0.01mol) and acetophenol hydrazine diphenyl phosphine methane (4a) (7.37g, 0.01mol) was dissolved in methanol, at 30^{0}C stirred well for 3 h using magnetic stirrer.

The obtained product was washed with acetone and recrystallized to increase the purity. The schematic diagram of synthesizing the newly diphenylphosphino methane complexes and their derivatives are illustrated in Fig. 1.

The solubility measurements were carried out at different temperatures. The transparent single crystals of apyrazole Cu-dppm (5a) were harvested after 20 days at 35 ^{o}C with accuracy of ±0.02^{o}C using constant temperature water bath. The solubility curve of Cu-dppm (5a) and the photograph of the grown crystal is shown in Fig. 2.

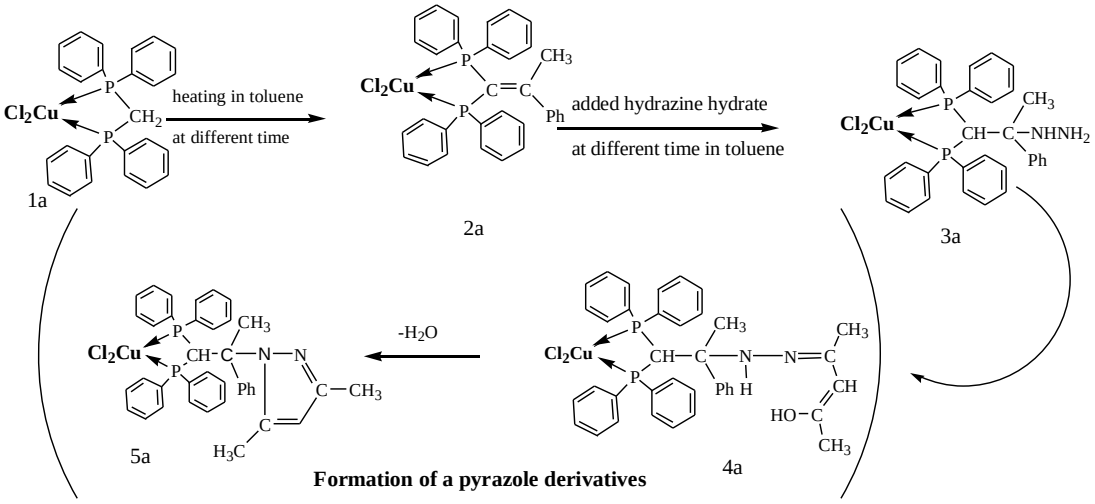

Fig. 1. Schematic diagram describes the formation of a pyrazole derivative

The formation of a pyrazole derivatives were prepared by elimination of one molecular water from the 4a $[Cl_2M\{(Ph_2P)_2CHCMe(Ph)NHN{=}C(CH_3)CH{=}C(OH)CH_3\}]$ complexes. Treatment of the [Cu-dppm] $(Cl)_2$ adduct in n-decane with a slight excess (20%) of phenyl acetone gave $[(Cl)_2Cu\{(Ph_2P)_2C{=}CMe(Ph)\}]$ after heating ca1h under dinitrogen, crystals of the copper complex adduct in >80% yield [15].

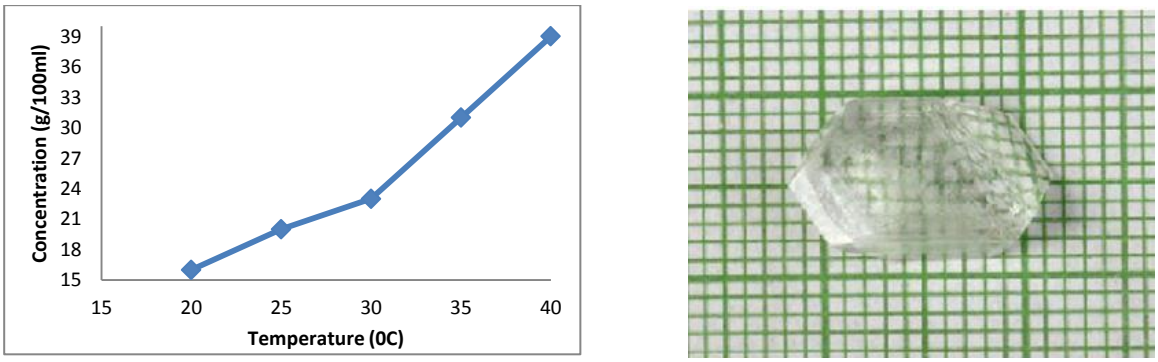

Fig. 2.Cu-dppm (5a) solubility curve and the photograph of the grown crystals at 35 ^{0}C.

2.2. Characterization techniques

The ^{1}H NMR spectrum was recorded using the "Varian Em-390-90MHz NMR spectrometer" using $CDCl_3$ as a solvent and TMS as an internal standard (chemical shifts in δ ppm).JEOL Gx 400 with chemical shifts relative to high frequency of residual solvent.

IR spectra were recorded in the range400–4000 cm^{-1} on a Shimadzu Corporation Chart 200-91527, using KBr pellets. The high-resolution X-ray diffraction curve (DC) was recorded for a typical complex Cu-dppm (5a) single crystal specimen using(-101) diffracting planes in symmetrical Bragg geometry by employing the multicrystal X-ray diffractometer with Mo $K\alpha_1$ radiation.

A "UV-visible double beam spectrophotometer of model UV-1650PC" was employed for recording the reflectance, transmittance and absorbance spectra over the incident photon energy of the wavelength range 400-800 nm.

2.3. Crystal structures refinement and determination

X-ray crystallographic study was carried out in the National Research Center, Cairo, Egypt. A white crystal of Cu-dppm (5a) complex having approximate dimensions of 1.31 x 0.42 x 0.91 mm^3 was mounted on a glass fiber in a random orientation.

The data collection was performed with Mo kα radiation of wavelength 0.71073 Å, on a Bruker – Nonius, Holland, computer controlled kappa axis diffractometer CCD, with computing data reduction of Denzo and Scale pack [16], Maxus [17], and the computing molecular graphics by Ortep [18] did the computing structure refinement and publication material. The reflection threshold expression is I > 3.00 Sigma (I). The crystal data and structure refinements are shown in Table 1.

Activation energies of the Cu-dppm (5a) complex are obtained from the slopes of the straight lines of the relation $\ln(\ln 1/C_s)$ versus θ, according to the equation [19]:

$$\ln(\ln\frac{1}{C_s}) = (W_o - W_t^f) = \frac{E^*\theta}{RT_s^2} \quad (1)$$

where W is the weight remaining at a given temperature T, W_o and W_t^f are the initial and final weights, respectively, C_s is the weight Cu-dppm (5a) complex after being converted to mole fraction, E* is the energy of activation ,and $\theta=T-T_s$, where T_s is the intermediate temperature of degradation.

Table 1. Crystal Data and Structure Refinements for Cu-dppm (5a) Complex.

Crystal data:		
$C_{38}H_{36}Cl_2CuN_2P_2$	D_x=1.512 gm cm^{-3}	Refinements
Mr= 717.11	Mo K_α radiation	Refinements on F^2
Monoclinic $P2_1/n$	Cell parameter from	$R[F^2>2\sigma(F^2)]$ 0.042
a=9.502 (2) *Å*	Reflections 2250	$wR(F_2)$= 0.122
b=8.128 (3) *Å*	θ = 2.18-67.91°	S= 1.077
c=16.112 (6) *Å*	μ = 4.493 mm^{-1}	999 reflections
v=1235.7 *Å*	White	122 parameters
z=4	0.3x0.2x0.2 mm^{-3}	
Data collection		
Kappa CCD	2250 independent reflection	H- atom parameters
diffractometer	999 reflection with I>2σ (I)	constrained
ϕ s and ω scans	R_{int}=.035	W= l/ [s^2 (F_0^2) +0.1
with Kappa offset scans	h = -11---11	F_0^2]
Absorption correct	k= 0-------9	$(\Delta/\rho)_{max}$= 0.37 e A^{-3}
not provided	l= -19-----19	$\Delta\rho_{max}$ = 0.782 e A^{-3}
2729 measured		$\Delta\rho_{min}$ = -0.719 e A^{-3}
reflections		

3. Results and discussion

3.1. Spectroscopic studies of organic crystalline semiconductors

Fig. 3 shows ^{1}H-NMR and ^{31}P-{^{1}H}NMR spectra (400MHz) of Cu-dppm (5a) complex, and also this complex consisted of a sharp singlet at δ=45.61p.p.m and value of ^{1}J(CuP)/Hz=zero. A five signals (excluding aromatic hydrogen) of ^{1}H -NMR which appears at δ=6.04p.p.m. a triplet of relative intensity 1H is observed and assigned to CH, ^{4}J(C<u>H</u>-C-C<u>H</u>$_3$)=2.72 Hz. A strong signal is centered at δ=1.08 p.p.m, of relative intensity 3H, assigned to (-CH-C-CH_3) protons. A singlet at δ= 5.57p.p.m of relative intensity 1H is observed, assigned to ethylene (–C=CH-) proton. A singlet at δ= 2.08p.p.m of relative intensity 3H is observed, assigned to (-N-N=C-CH_3-) proton. A singlet at δ= 2.71 p.p.m of relative intensity 3H is observed, assigned to (-N-C-CH_3=CH-) proton, and the ^{1}H -NMR spectrum coupling to phosphorus is shown by the protons CH, ^{2}J(<u>P</u>C<u>H</u>^{1})=12Hz.

Table 2. ^{31}P-{^{1}H}-NMR. data[a], and Infrared data[b] for some Condensation of [$(Cl)_2Cu\{(Ph_2P)_2CH_2\}$]

Complex	δ(P) p.p.m	(ν Cu-Cl) and (υ P-C)/cm^{-1}	υ(NH)/cm^{-1}
$C_{25}H_{22}Cl_2CuP_2$: 1a	45.08	310s, 295s single band (ν Cu-Cl) 725s, 690s single band (ν P-C)	-
$C_{33}H_{28}Cl_2CuP_2$: 2a	45.38	320s, 285s single band (ν Cu-Cl) 710s, 690s single band (ν P-C)	-
$C_{33}H_{32}Cl_2N_2CuP_2$: 3a	43.24	325s, 290s single band (ν Cu-Cl) 715s, 680s single band (ν P-C)	3350
$C_{38}H_{38}Cl_2N_2CuOP_2$: 4a[C]	45.61	314s, 285s single band (ν Cu-Cl) 710s, 685s single band (ν P-C)	3300
$C_{38}H_{36}Cl_2N_2CuP_2$: 5a	45.93	315s, 290s single band (ν Cu-Cl) 720s, 680s single band (ν P-C)	-

a) Chemical shifts, δ, to high frequency of 85% H_3PO_4; b) Far infrared in KBr discs and c) υ(OH) = 3240 cm^{-1}.

The IR spectra of Cu-dppm (5a) complex are recorded as shown in Table 2. The comparison between IR spectrum of (4a) and Cu-dppm (5a) complex spectrum shows that there is a change of position in the corresponding vibrations. The strong absorption peaks showed υ(NH) at 3300cm^{-1} and showed υ(OH) at 3250 cm^{-1}.

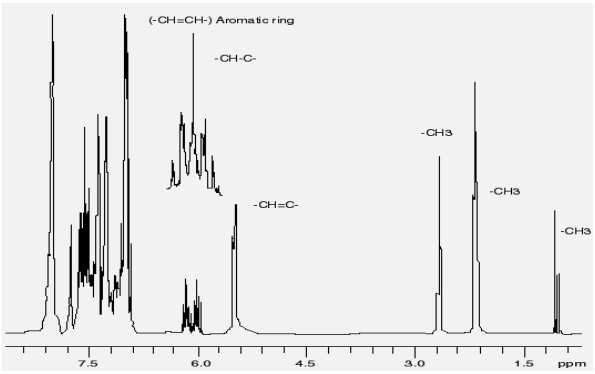

Fig. 3. The ^{1}H-{^{31}P} and ^{1}H NMR spectra for the Cu-dppm (5a) crystals.

3.2. Single crystal X-ray studies

A wide variety of adducts formed between group 11 metal-halides, $CuCl_2$ and unidentate diphosphorous bases have been characterized by room-temperature single crystal X-ray studies. Single crystals suitable for X-ray crystallographic analysis are selected following examination under a microscope. X-ray intensity data of 2729 reflections are collected on 'X' caliber CCD area-detector diffractometer equipped with graphite monochromated Mo K_α radiation. The cell dimensions are determined by least-squares fit of angular settings of 2729 reflections in the θ range 2.18-67.9°. Cu-dppm (5a) crystallizes in monoclinic system with space group $P2_1/n$. The crystallographic details of data collection and the structure refinement parameters of the compound are presented in Table 1. Selected bond length and bond angles of the complex Cu-dppm (5a) are shown in Table 3 **a**nd Fig.. 4a,b.

Table 3. Selected Bond Lengths (Å) and Angles (°) of Cu-dppm Organic Semiconductor.

Bond	(Å)	Bond	(Å)	Bond	Angles (°)	Bond	Angles (°)
P(1)-C(15)	1.846	N(30)-C(31)	1.257	C(15)-P(1)-Cu(17)	91.743	P(1)-C(15)-P(3)	89.997
P(1)-Cu(17)	2.302	N(30)-N(43)	1.426	C(15)-P(1)-C(24)	102.534	P(1)-C(15)-C(44)	111.527
P(1)-C(24)	1.786	C(31)-C(32)	1.513	Cu(17)-P(1)-C(24)	144.274	H(16)-C(15)-C(44)	118.330
P(1)-C(25)	1.785	C(31)-C(35)	1.574	Cu(17)-P(1)-C(25)	106.109	P(1)-Cu(17)-P(3)	71.756
C(2)-P(3)	1.785	C(32)-C(34)	1.327	C(24)-P(1)-C(25)	102.607	P(1)-Cu(17)-Cl(55)	109.5007
P(3)-C(4)	1.785	C(32)-H(33)	1.118	P(3)-C(2)-C(10)	120.000	Cl(55)-Cu(17)-Cl(56)	131.426
P(3)-C(15)	1.785	C(34)-C(39)	1.497	C(2)-P(3)-C(4)	102.927	C(31)-N(30)-N(43)	104.5073
P(3)-Cu(17)	2.314	C(34)-N(43)	1.472	C(2)-P(3)-Cu(17)	109.711	N(30)-C(31)-C(32)	111.005
C(15)-C(44)	1.486	N(43)-C(44)	1.475	C(4)-P(3)-C(15)	102.085	N(30)-C(31)-C(35)	121.348
C(15)-H(16)	1.207	C(44)-C(45)	1.541	C(4)-P(3)-Cu(17)	142.108	C(34)-N(43)-C(44)	108.370
Cu(17)-Cl(55)	2.098			C(15)-P(3)-Cu(17)	89.997	C(32)-C(34)-N(43)	103.934
Cu(17)-Cl(56)	2.204			P(3)-C(4)-C(9)	119.798	C(39)-C(34)-N(43)	130.101
				N(30)-N(43)-C(34)	111.002	N(43)-C(44)-C(45)	110.740
				N(30)-N(43)-C(44)	119.962	C(15)-C(44)-N(43)	110.740

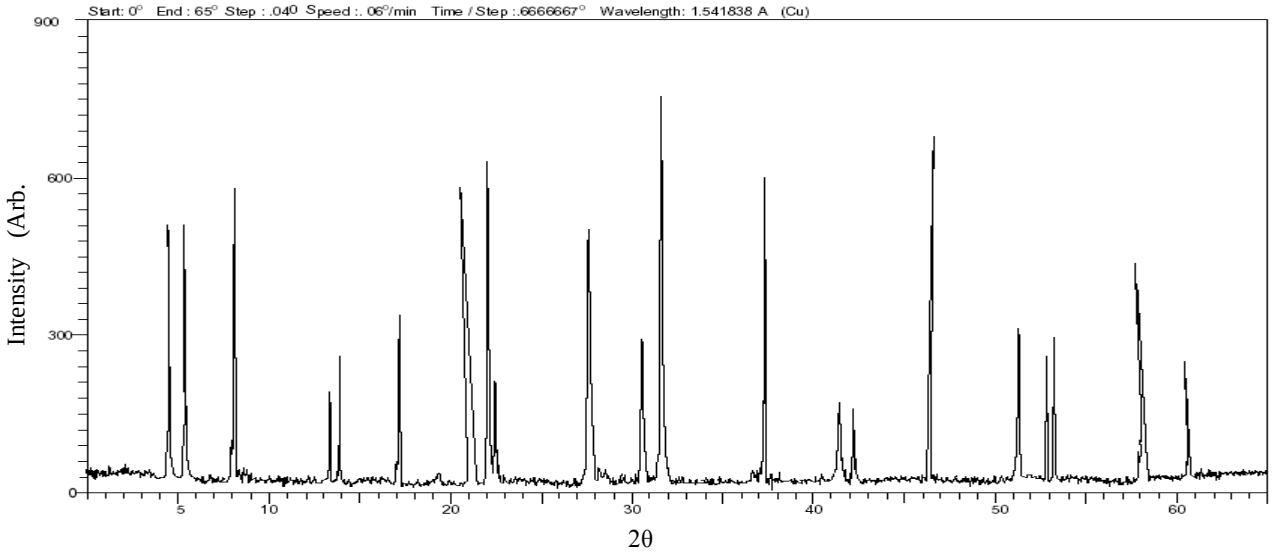

Fig..4a. Powder X-ray diffraction (XRD) pattern of Cu-dppm (5a) crystal.

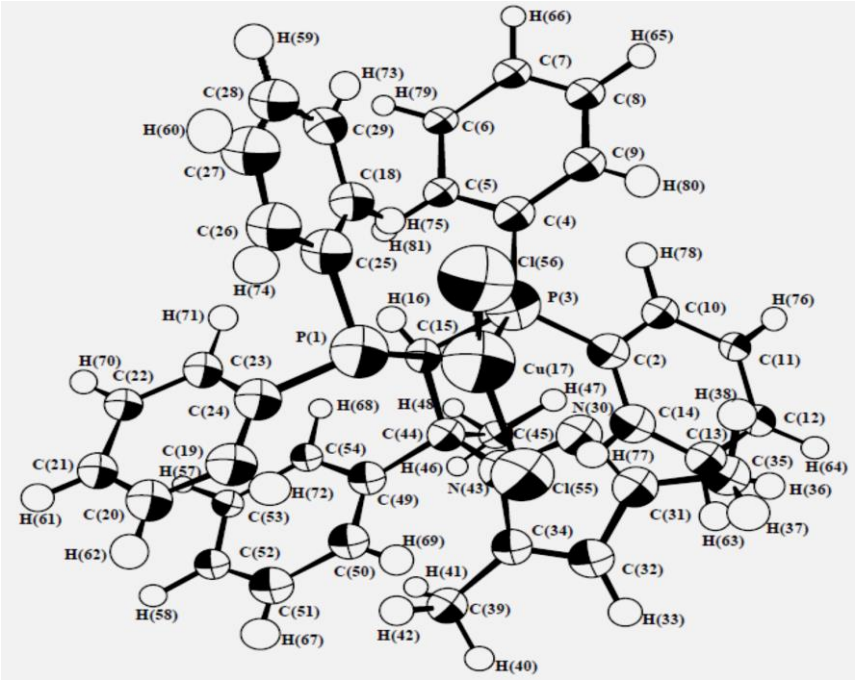

Fig. 4b.The molecular geometry with the atom-numbering scheme.

Bragg's Law, d=λ/(2sinθ), supports a minimum size of measurement of λ/2 in a diffraction experiment (limiting sphere of inverse space) but does not predict a maximum size. The well-defined intense peaks of Cu-dppm organic semiconductor crystal(5a) shown in Fig..4b reveals the crystalline nature of the sample and the prominent peaks present at different angles explain the planes present in the crystals. The obtained values are in good agreement with the single crystal X-ray diffraction data (as shown in Table 4).

Table 4. Single Crystal and Powder X-ray Diffraction (XRD) report on Cu-dppm (5a) Organic Semiconductor Crystal.

Crystallographic lattice parameters	Data of single crystal XRD	Date of powder XRD
a (Å)	9.502 (2)	9.4975± 0.0241
b (Å)	8.128 (3)	8.128± 0.0121
c (Å)	16.112 (6)	16.104± 0.072
α(o)	90	90
β(°)	97.324 (3)	97.324
γ(°)	90	90
v(A^3)	1235.7	1234.9

3.3. Optical absorption studies in the newly Cu-dppm organic semiconductor

The UV–Vis–NIR spectrum gives information about the structure of the molecule because the absorption of UV and visible light involves the promotion of the electron in σ and π orbital from the ground state to higher energy states. UV spectral analysis is important for any organic semiconductor, because a non-linear optical material is of great practical use only if it has a wide transparency window.

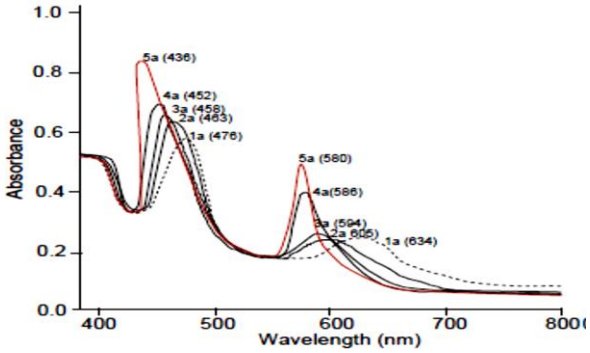

Fig..5. UV–vis spectrum of Cu-dppm organic semiconductor crystal.

As it is clear from Fig. 5 that the crystal has UV cut off wavelength at 436nm for sample 5a. The grown crystal possesses high transmittance in the visible region, which could be useful for optical window applications. This provides sufficient optical window for second harmonic generation (SHG) laser radiation or other application in the blue region [20]. The absorption coefficient (α) was calculated from the transmittance data (T) using the relation [21].

$$\alpha = \frac{ln\left(\frac{1}{T}\right)}{t}, \tag{2}$$

where T is the transmittance and t is the thickness of the sample.

The electronic absorption spectral data (λ_{max} and ε_{max} values) for the synthesized diphosphine derivatives cupper complexes 1a, 2a, 3a, 4a and 5a in dichloromethane is reported in Table 5.

Table 5. The values λ_{max}/nm and (ε_{max}/Lmol-1Cm-1) for Phosphino-substituted Hydrazine Copper Complexes in CH_2Cl_2.

Compound		λ_{max}/nm(ε_{max}/Lmol^{-1}Cm^{-1})	λ_{max}/nm(ε_{max}/L mol^{-1}Cm^{-1})
1a	$C_{25}H_{22}Cl_2CuP_2$	476 (334.28)	634 (394.79)
2a	$C_{33}H_{28}Cl_2CuP_2$	463 (722.6)	605 (301.96)
3a	$C_{33}H_{32}Cl_2N_2CuP_2$	448 (895.18)	594 (343.89)
4a	$C_{38}H_{38}Cl_2N_2CuOP_2$	452 (1129.50)	586 (443.94)
5a	$C_{38}H_{36}Cl_2N_2CuP_2$	436 (729.95)	580 (349.39)

Absorption spectra of the investigated Cu-dppm (5a) complex doped with transition element (copper) exhibit double absorption bands within the wavelength range (λ=400-800 nm) in CH_2Cl_2 solvent. One with the position of the absorption maximum (λ_{max}= 436 nm) being responsible for n-π transition in aromatic rings and the second having (λ_{max}= 580 nm) which attributed to π-π* in (-N-N= group) in a pyrazole ring [30-31]. However, in the case of compounds without a pyrazole ring λ_{max} towards higher energy region was significantly hypsochromically shifted depending on the nature of the aliphatic and aromatic aldehydes and ketones. Considering the influence of the dielectric constant of solvent on value of λ_{max}.

The optical band gap is calculated using the following relation:

$$\alpha h\upsilon = A(h\upsilon - E_g)^m \tag{3}$$

where, A is a constant depends on the transition probability and the value of E_g and m depends on the energy and the nature of the particular optical transition with absorption coefficient (α). Moreover, m is an exponent that characterizes the type of the optical transition in the Cu-dppm semiconductor organic crystals. For allowed direct, allowed indirect, forbidden direct and forbidden indirect transitions, the value of m corresponds to 1/2, 2, 3/2 and 3, respectively [22].

ted to determine the value of m without pre-assuming the nature of the optical transition in the crystal. Now, Eq. (3) can be rewritten as [23]

$$\frac{d[\ln(\alpha h\upsilon)]}{d(h\upsilon)} = \frac{m}{h\upsilon - E_g} \tag{4}$$

From the equation 4 a discontinuity at a particular value hυ=E. Where a possible optical transition might have occurred corresponding to a particular band gap E=2.23 ev for Cu-dppm crystal.

In order to get the m value corresponding to the optical transition at 2.23eV, we plot ln(αhυ) as a function of ln(hυ)-E), where E = 2.23 eV for the optical transition as shown in Fig. 6a. The slope of the plot is determined by performing a linear fitting of the experimental data. The slope is quite near to 0.5 is observed. This confirms that the type of optical transition in Cu-dppm crystal is of allowed direct nature.

The direct optical band gap of the Cu-dppm crystal is also determined by plotting $(\alpha h\upsilon)^2$ against the photon

energy (hυ).The relation between the optical absorption coefficient (α) for a direct transition and the photon energy (hυ) is given by [24-25]:

$$\alpha h\upsilon = A(h\upsilon - E_g)^{1/2} \quad (5)$$

The plot of $(\alpha h\upsilon)^2$ vs. (hυ) for the Cu-dppm crystal is shown in Fig. 6b. The value of the optical energy gap E_g is determined from the intersection of the extrapolated line with the photon energy axis (at $(\alpha h\upsilon)^2 = 0$). The direct optical band gap of the ***Cu-dppm*** crystal is found to be 2.16 eV

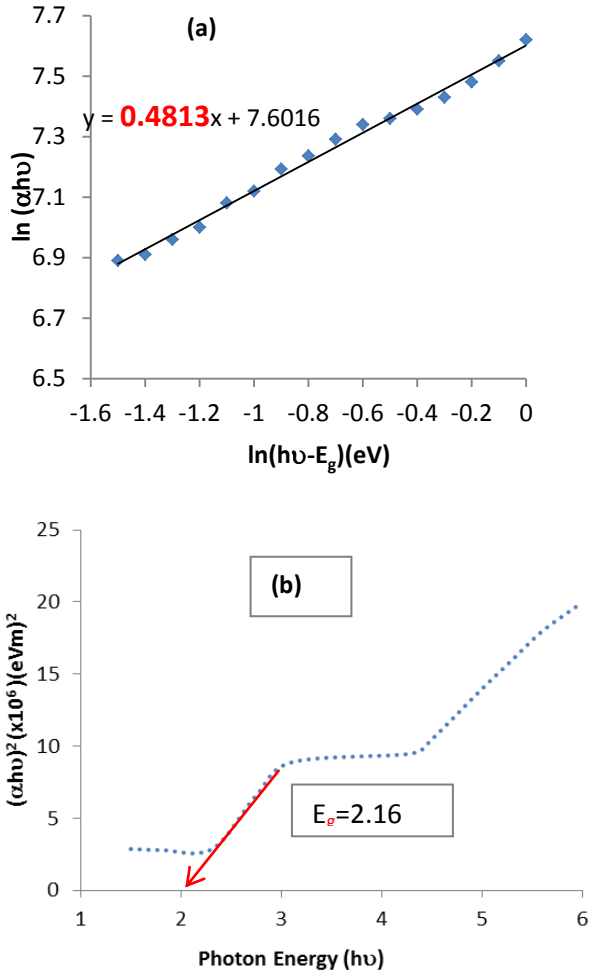

Fig. 6. (a) Linear fit of ln(αhυ) vs. ln(hυ-Eg) where Eg=2.23eV, (b) $(\alpha h\upsilon)^2$ vs. hυ plot for Cu-dppm crystal.

The refractive index can be determined from the reflectance (R) and transmittance (T) data using the relation [26-27]

$$R = \frac{(n-1)^2}{(n+1)^2} \quad (6)$$

$$T = \frac{(1-R)^2 \exp(-\alpha t)}{1 - R^2 exp\,(-2\alpha t)} \quad (7)$$

From this equation the reflectance (R) in terms of the absorption coefficient can be obtained and is given by

$$R = \frac{\exp(-\alpha t) \pm \sqrt{\exp(-\alpha t)\,T - \exp(-3\alpha t)\,T + \exp(-2\alpha t)\,T^2}}{\exp(-\alpha t) + \exp(-2\alpha t)\,T} \quad (8)$$

The refractive index (n) can be determined from the reflectance (R) data using the equation [28]

$$n = \frac{-(R+1) \pm 2\sqrt{R}}{(R-1)} \quad (9)$$

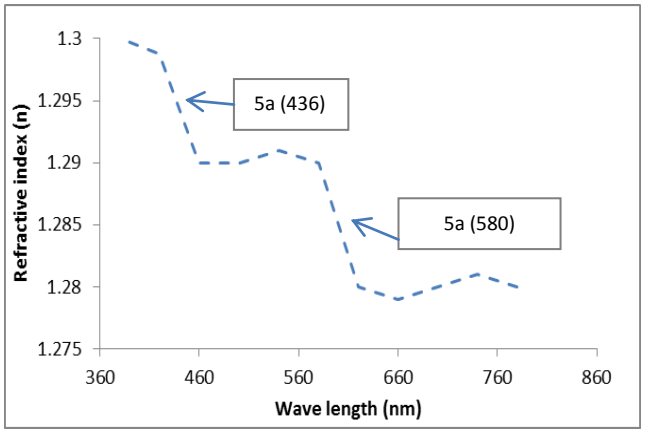

Fig.7. Refractive index vs. wavelength for Cu-dppm crystal.

Fig.7 shows the variation of refractive index with wavelength. It is noticed that the Cu-dppm organic semiconductor crystal has positive refractive index (n=1.265 at λ=436 nm) with respect to photon energy and this reveals the focusing nature of the crystal. It is clear that the refractive index of Cu-dppm organic semiconductor crystal depends on photon energy and by tailoring the photon energy one can achieve the desired material to fabricate the optoelectronic devices [29]. A long tails in the low energy region, where a week absorption tail is most probably originated from defects and impurity states within the band gap. Tailing of the band states into the gap width may also be induced from a large concentration of free carriers resulting from screened Coulomb interaction between carriers that perturbs the band edges.

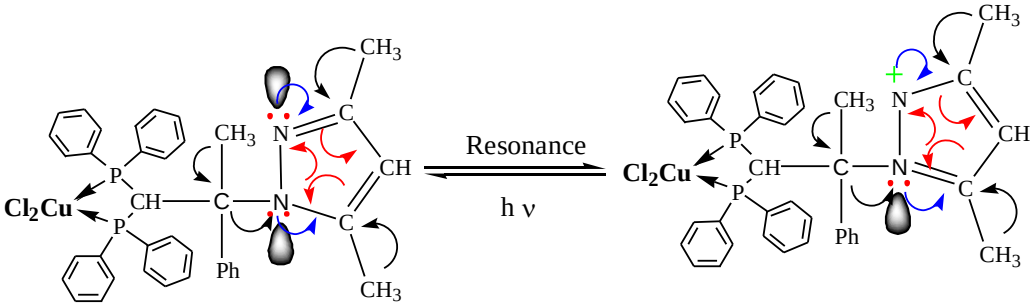

Fig. 8. Resonance of (5a) Cu-dppm organic semiconductor crystal.

The delocalization process of electrons within certain molecules in Cu-dppm crystal (resonance) is shown in Figure 8. It is observed that, the resonance structures of Cu-dppm (5a) are characterized by its properties of position, intensity, shape, and fine structure.

4. Conclusion

It has been demonstrated that the Cu-dppm (5a) complex by Micheal addition reaction showed a good rectifying behavior. Moreover, five a pyrazole derivatives were obtained and investigated structurally by elemental analysis (EA), IR, ^{1}H-NMR, ^{31}P-NMR spectroscopic data, FAB mass spectra and X-ray single crystal. Cu-dppm (5a) crystallizes in monoclinic system with space group $P2_1/n$. Moreover, short bond C(32)-H(33) equal to 1.118 Å and short angle equal to 71.756^{o}.

The Apyrazole derivatives for diphenylphosphino-methane-Cu-dppm Hydrazine complexes $C_{38}H_{36}Cl_2N_2CuP_2$ shows typical semiconductor behavior due to the delocalization of the π-electrons in the structure (5a) complex. The transmittance and reflectance spectra were used for investigating the charge transports and optical parameters of the Cu-dppm organic crystalline semiconductors.

All optical measurements were carried out in the incident photon energy range 1.40 to 2.64eV. By using the energy dependence of the absorption coefficient, it was clear that in the short wavelength region, the absorption coefficient linearly increases for the Cu-dppm crystals with the increase in the incident photon energy. In addition, the optical measurements exhibit direct allowed transitions in the Cu-dppm organic crystals.

References

[1] R.H. Friend, R. W. Gymer, A. B. Holmes, J. H. Burroughes, R. N. Marks, C. Taliani, D.C. Bradley, D.A. Dos Santos, J. Br´edas, M. Logdlund, W.R. Salaneck,. Nature, **397,** 121 (1999)

[2] H. Sirringhaus, P.J. Brown, R.H. Friend, M.M. Nielsen, K. Bechgaard, B.M.W. Langeveld-Voss, A.H. Spiering, R.A.J. Janssen, E.W. Meijer, P. Herwig, D.M. De Leeuw, Nature, **401**, 685 (1999)

[3] T. Someya, A. Dodabalapur, J. Huang, K.C. See, H.E. Katz, Advanced Materials**,** **22**(34), 3799 (2010).

[4] B. Crone, A. Dodabalapur, Y. Y. Lin, R. W. Filas, Z. Bao, A. LaDuca, R. Sarpeshkar, H.E. Katz, W. Li, Letters to Nature, **403**, 521 (2000).

[5] J. Thomas Joseph Prakash, N. Vijayan, S. Kumararaman, Cryst. Res. Technol, **43**, 428 (2008).

[6] G. Malliaras, Physics Today, **58**(5), 53 (2005).

[7] J. Cui, A.P. Beyler, T.S. Bischof, M.W.B. Wilson, M.G. Bawendi, Chemical Society Reviews, **43,** 1287 (2014).

[8] E. Piorkowska, G. C. Rutledge, Handbook of polymer crystallization, John Wiley & Sons, (2013).

[9] R.C.G. Naber, B. De Boer, P.W.M. Blom, D.M. De Leeuw, Appl. Phys. Lett.**, 87,** 203509 (2005).

[10] M. Yun, A.Sharma, C. Fuentes-Hernandez, D.K. Hwang, A. Dindar, S. Singh, S. Choi, B. Kippelen, ACS Appl. Mater. Interfaces, **6**(3),1616 (2014).

[11] X. Guo, J.P. Small, J.E. Klare, Y. Wang, M.S. Purewal, I.W. Tam, B.H. Hong, R. Caldwell, L. Huang, S.O. Brien, J.J. Yan, R. Breslow, S.J.Wind, J. Hone, P. Kim, C. Nuckolls, Science, **311**, 356 (2006).

[12] A. Bonfiglio, D. De. Rossi, T. Kirstein, I.R. Locher, F. Mameli, R. Paradiso, G. Vozzi, Tech. in Biomed, **9**, 319 (2005).

[13] S. F. Forrest, Nature, **428**, 911 (2004).

[14] A.M. Badr, A.A. EL-Amin, A.F. Al-Hossainy, Eur. Phys. Journal B, **53,** 439 (2006).

[15] A.M. Badr, A.A. EL-Amin, A.F. Al-Hossainy, Journal Phys. Chem. C, **112**(36), 14188 (2008).

[16] Z. Otwinowski, W. Minor, In Methods in Enzymology, **276**, Edit. By Carter, C.W. Sweet, R.M. p. 307, New York: Academic Press, 1976.

[17] S. Mackay, C.J. Gilmore, C. Edwards, N. Stewart, Shankland, K. Maxus, The Netherlands, MacScience, Japan &The University of Glasgow, 1999.

[18] C. K. Johnson, ORTEP-II.A Fortran Thermal-Ellipsoid Plot Program, Report ORNL-5138. Oak Ridge National Laboratory, Oak Ridge, Tennessee, USA, 1976.

[19] N. Renukaa, N. Vijayan, R. Brijesh Rathi, K.

Ramesh Babu, D. Nagarajan, G.B. Haranath, Optik **123,** 189 (2012).
[20] C.N.R. Rao, Ultraviolet and Visible Spectroscopy, 3rd Ed., Butter worths, London, (1975).
[21] A. Ashour, Turk J Phys., **27**, 551 (2003).
[22] A.B.Murphy, Solar Energy Materials and Solar Cells, **91**(6), 1326 (2007)
[23] A. Somik Banerjee, A. Kumar, Nucl. Instrum. Methods Phys. Res. B, **269,** 2798 (2011).
[24] K. Russel Raj, P. Murugakoothan, Optik, **123,** 1082 (2011).
[25] L. Fraas, L. Partain, Solar Cells and their applications, John Wilry & Sons, 2010.
[26] B.K. Ridley, Quantum processes in semiconductors, 5th Ed., Oxford University press, 2013.
[27] B.K. Periyasmay, R.S. Periyasamy, N. Jebas, T. Gopalakrishnan, Mat. Lett., **61**(21), 4246 (2007).
[28] T. Arumanayagam, P. Murugakoothan, Journal of Crystal Growth**, 362,** 304 (2013).
[29] A. Lucarelli, S. Lupi, P. Calvani, P. Masellr, G. De Marzi, P.,Roy, Saim, N.L.A. Bianconi, T. Ito, K. Oka, Phys. Rev. B, **65,** 54511 (2002).
[30] R.M. Abd El–Aal, A.A.M. Belal, Dyes and Pigments, **65,** 129 (2005).
[31] B. Karami, S. Khodabakhshi, K. Eskandari, Tetrahedron Letters, **53**(12), 1445 (2012).

*Corresponding author: af_73chem@hotmail.com